

A Particle Method without Remeshing

Matthias Kirchhart*

Christian Rieger†

Abstract

We propose a simple tweak to a recently developed regularisation scheme for particle methods. This allows us to choose the particle spacing h proportional to the regularisation length σ and achieve optimal error bounds of the form $\mathcal{O}(\sigma^n)$, $n \in \mathbb{N}$, without any need of remeshing. We prove this result for the linear advection equation but also carry out high-order experiments on the full Navier–Stokes equations. In our experiments the particle methods proved to be highly accurate, long-term stable, and competitive with discontinuous Galerkin methods.

Keywords: particle methods; numerical analysis; computational fluid dynamics; level-set method

1 Introduction

The convergence of many classical, uniform discretisations of partial differential equations is often governed by only two parameters: the discretisation order $n \in \mathbb{N}$ and the underlying mesh-size $\sigma > 0$. Assuming that the exact solution is smooth enough, one typically obtains error bounds of the type $\mathcal{O}(\sigma^n)$.^[1, Theorem (5.4.8)] Particle methods like Smoothed Particle Hydrodynamics (SPH) or Vortex Methods (VM), on the other hand, feature *two* orders $n, m \in \mathbb{N}$ and *two* sizes $h, \sigma > 0$. Here, h describes some form of particle spacing and m the order of an underlying quadrature rule, while on the other hand σ describes a smoothing length and n the order of a regularisation scheme. These parameters need to be very carefully chosen to ensure convergence. Typical error estimates for solutions to, e. g., the linear advection equation read:^[2, Theorem 4.2]

$$\|u - u_{h,\sigma}\|_{L^p(\Omega)} = \mathcal{O}\left(\sigma^n + \left(\frac{h}{\sigma}\right)^m\right). \quad (1)$$

For fixed values of n , m , and σ , the optimal choice of h thus is a compromise that balances both contributions. In the case $n = m$, this results in $h \sim \sigma^2$; in other words the particle spacing h needs to be negligible compared to the smoothing length. In practice this often is prohibitively expensive. An alternative is to ‘cheat’ and set $m = \infty$: on first sight this would allow for choosing $h \sim \sigma^{1+\varepsilon}$ for any $\varepsilon > 0$, i. e., h could essentially be chosen proportional to σ . However, the constants hidden in the \mathcal{O} -notation very quickly grow with m and time t , and thus also make this approach infeasible in practice. For this reason current particle methods typically have to *remesh* the particles to their original locations after every other time-step or so. But particle approximations are *exact solutions* of the advection equation, in a sense that will be made clear in [Subsection 2.2](#). Apart from destroying the purely Lagrangian character of the method, the remeshing process deviates from this exact solution and thereby introduces further errors.

In this work we describe a surprisingly simple tweak to a recently developed regularisation scheme, enabling us to chose $h \sim \sigma$ and m independent of n while still yielding the optimal error bound of $\mathcal{O}(\sigma^n)$. In our numerical experiments this difference turned out to be dramatic and enabled us to perform long-term simulations without remeshing.

*Centre for Computational Engineering Science, Mathematics Division, RWTH Aachen University. Schinkelstraße 2, 52062 Aachen, Germany. E-Mail: kirchhart@mathcces.rwth-aachen.de

†Institute for Numerical Simulation, University of Bonn. Endenicher Allee 196, 53115 Bonn, Germany. rieger@ins.uni-bonn.de

The rest of this article is structured as follows. In [section 2](#) we review ‘classical’ particle methods and some of the key results from their analysis. In [section 3](#) we give references to the literature for further reading and related results. [Section 4](#) is the core of this article: we describe a simple tweak to a recently proposed scheme: particle regularisation by projection onto spline spaces. A complete convergence analysis for the linear advection equation is provided. Finally, in [section 5](#) we carry out numerical experiments for the full, non-linear Navier–Stokes equations. For simplicity, throughout this article we restrict ourselves to the geometry of an axis-aligned cube, but point out that the regularisation scheme also generalises to the case of domains with arbitrary Lipschitz boundary. We conclude with some remarks on remaining open problems and possible future extensions.

2 Particle Methods

In this section we recall the necessary ingredients to describe particle methods. For a rigorous derivation of these results the reader is referred to Raviart’s lecture notes.^[2]

2.1 Linear Advection Equation

In order to keep our focus on the problem at hand, we will discuss particle methods in one of the simplest possible settings: the linear advection equation in the box. Thus let $\Omega := (0, 1)^D$, typically $D \in \{2, 3\}$. Let $\mathbf{a} : \Omega \times [0, T] \rightarrow \mathbb{R}^D$ denote a given smooth and bounded velocity field that—for simplicity—also satisfies $\nabla \cdot \mathbf{a} \equiv 0$ and $\mathbf{a} \cdot \mathbf{n} = 0$ on $\partial\Omega$. Given continuous initial data $u_0 \in C(\Omega)$, we are looking for the solution $u : \Omega \times [0, T] \rightarrow \mathbb{R}$ of the following initial value problem:

$$\begin{cases} \frac{\partial u}{\partial t} + (\mathbf{a} \cdot \nabla)u = 0 & \text{in } \Omega \times [0, T], \\ u(\mathbf{x}, 0) = u_0(\mathbf{x}) & \text{on } \Omega. \end{cases} \quad (2)$$

Throughout this article we demand continuity of the initial data, such that point-wise evaluation is well-defined. It is well-known that problem (2) can be solved by the method of characteristics. Thus, for any $(\mathbf{x}, \tau) \in \Omega \times [0, T]$ let us define the *trajectory* $\mathbf{X}(t; \mathbf{x}, \tau)$ as the solution of the following initial value problem:

$$\begin{cases} \frac{d\mathbf{X}}{dt}(t; \mathbf{x}, \tau) = \mathbf{a}(\mathbf{X}(t; \mathbf{x}, \tau), t), \\ \mathbf{X}(\tau; \mathbf{x}, \tau) = \mathbf{x}. \end{cases} \quad (3)$$

By the Picard–Lindelöf theorem one obtains that \mathbf{X} is well-defined. Moreover, it can be shown that the map $\Phi_\tau^t(\mathbf{x}) := \mathbf{X}(t; \mathbf{x}, \tau)$ is a diffeomorphism with inverse Φ_t^τ . Colloquially speaking $\Phi_\tau^t(\mathbf{x})$ tells us where the particle with position \mathbf{x} at time τ will be at another time t . The solution to the advection equation (2) then is given by $u(\mathbf{x}, t) = u_0(\Phi_t^0(\mathbf{x}))$.^[2, Equation (1.11)]

In the lecture notes of Raviart^[2] the theory is then extended to weak solutions in Sobolev spaces and it is shown that the solutions are bounded, i. e.:

$$\|u(\cdot, t)\|_{W^{s,p}(\Omega)} \lesssim \|u_0\|_{W^{s,p}(\Omega)} \quad t \in [0, T], \quad s \in \mathbb{R}, \quad p \in [1, \infty]. \quad (4)$$

Throughout this article the symbol C refers to a generic constant $C > 0$ that is independent of h , σ , and the functions occurring in the norms. The notation $a \lesssim b$ means $a \leq Cb$ for some $C > 0$, and $a \sim b$ means $a \lesssim b \lesssim a$. In estimate (4), for example, the hidden constant depends on \mathbf{a} and T , but is independent of $u(\cdot, t)$, u_0 , and t .

2.2 Particle Approximations

A simple, intuitive approach to numerically solving the advection equation (2) could consist of storing samples $u_i := u_0(\mathbf{x}_i)$ of the initial data u_0 at a finite set of locations $\mathbf{x}_i \in \Omega$, $i = 1, \dots, N$. One could

then track these *particles* over time by solving $\dot{\mathbf{x}}_i(t) = \mathbf{a}(\mathbf{x}_i(t), t)$ by means of, e. g., a Runge–Kutta method. We then know that at any time t we have $u(\mathbf{x}_i(t), t) = u_i$. The question that then arises, however, is what happens in-between the particles. One could, of course, devise interpolation schemes, but these do not easily generalise to general bounded domains.

A related idea involves quadrature rules. Let us subdivide the domain $\Omega = (0, 1)^D$ into uniform squares/cubes of edge length h . To each of these cells we can apply a quadrature rule of polynomial exactness degree $m - 1$ with positive weights, e. g., Gauß–Legendre rules. This yields a set of nodes \mathbf{x}_i with associated weights w_i , $i = 1, \dots, N$. Furthermore setting $u_i := u_0(\mathbf{x}_i)$, $i = 1, \dots, N$, and letting δ denote the Dirac delta distribution, the functional $u_h(t = 0) := \sum_{i=1}^N w_i u_i \delta_{\mathbf{x}_i}$ approximates u_0 in the sense that for smooth functions φ it holds that:

$$\langle u_h(0), \varphi \rangle = \sum_{i=1}^N w_i u_i \varphi(\mathbf{x}_i) \approx \int_{\Omega} u_0 \varphi \, d\mathbf{x}. \quad (5)$$

This approach has the advantage that error-bounds are readily available. To avoid technicalities, let us for simplicity assume that $m \geq D$, such that by the Sobolev embedding theorem functions from $W^{s,p}(\Omega) \hookrightarrow C(\Omega)$ are continuous for all $m \geq s \geq D$, $p \in [1, \infty]$. The following bound then is a simple consequence of the Bramble–Hilbert lemma:^[1, Lemma (4.3.8)]

$$\|u_h(0) - u_0\|_{W^{-s,p}(\Omega)} \lesssim h^s \|u_0\|_{W^{s,p}(\Omega)} \quad m \geq s \geq D, \quad p \in [1, \infty]. \quad (6)$$

The *exact solution* to the advection equation (2) with u_0 replaced by $u_h(0)$ is again given by moving the particles according to $\dot{\mathbf{x}}_i(t) = \mathbf{a}(\mathbf{x}_i(t), t)$. Together with the stability estimate (4) this immediately yields:

$$\|u_h(t) - u(t)\|_{W^{-s,p}(\Omega)} \lesssim h^s \|u_0\|_{W^{s,p}(\Omega)} \quad m \geq s \geq D, \quad p \in [1, \infty]. \quad (7)$$

The problem here, however, is even worse. In fact, u_h is an irregular distribution that cannot be interpreted as an ordinary function. Even at the particle locations, we strictly speaking do not have function values, but only weights $w_i u_i$.

On paper the two approaches are of course somehow equivalent: it is trivial to obtain the function value u_i from the weight $w_i u_i$ and vice versa. But on the one hand, the first approach yields function values but does not allow us to perform numerical integration, while in the second approach the situation is reversed.

2.3 Particle Regularisation

Particle regularisation refers to the process of obtaining a function $u_{h,\sigma}$ from a given particle approximation u_h that is interpreted as a quadrature rule. The most common approach uses mollification and is more easily explained in the whole-space case $\Omega = \mathbb{R}^D$. Let $\zeta : \mathbb{R}^D \rightarrow \mathbb{R}$ be a smooth function that fulfils $\int_{\mathbb{R}^D} \zeta(\mathbf{x}) \mathbf{x}^\alpha \, d\mathbf{x} = \mathbf{x}^\alpha|_{\mathbf{x}=0}$ for all multi-indices $|\alpha| < n$ and some fixed $n \in \mathbb{N}$. In other words, for $|\alpha| < n$, convolution of \mathbf{x}^α with ζ behaves like convolution with the Dirac delta distribution: $(\zeta \star \mathbf{x}^\alpha) = (\delta \star \mathbf{x}^\alpha) = \mathbf{x}^\alpha$ and in this sense $\zeta \approx \delta$. Furthermore, for stability, it should hold that $\int_{\mathbb{R}^D} |\mathbf{x}|^n |\zeta(\mathbf{x})| \, d\mathbf{x} < \infty$. A multitude of such *kernel* or *blob functions* is available in the literature.^[3, Section 2.3] After choosing ζ and some $\sigma > 0$ one scales $\zeta_\sigma(\mathbf{x}) := \sigma^{-D} \zeta(\frac{\mathbf{x}}{\sigma})$. Finally, because $u_h \approx u$ and $\zeta_\sigma \approx \delta$ one obtains $u = u \star \delta \approx u_h \star \zeta_\sigma =: u_{h,\sigma}$, that is:

$$u_{h,\sigma}(\mathbf{x}, t) := \sum_{i=1}^N w_i u_i \zeta_\sigma(\mathbf{x} - \mathbf{x}_i(t)). \quad (8)$$

A careful analysis then reveals the aforementioned error bound:^[2, Theorem 4.2]

$$\|u(\cdot, t) - u_{h,\sigma}(\cdot, t)\|_{L^p(\Omega)} \lesssim \left(\sigma^n + \left(\frac{h}{\sigma} \right)^m \right) \|u_0\|_{W^{\max\{n,m\},p}(\Omega)}. \quad (9)$$

The origin of the $(\frac{h}{\sigma})^m$ -term lies in the quadrature error estimate (6). On the left the error is measured in the $W^{-m,p}$ norm, on the right we have the $W^{m,p}$ norm, i.e., a difference of $2m$ orders. Yet, the quadrature error is only $\mathcal{O}(h^m)$ as opposed to $\mathcal{O}(h^{2m})$. Because of Bakhvalov's theorem,^[4] the $\mathcal{O}(h^m)$ bound is asymptotically optimal and cannot be improved. This ultimately forces one to choose $h \ll \sigma$.

3 The Proposed Method in Context of the Literature

Vortex methods are the oldest particle methods and can at least be traced back to the early 1930s, when Rosenhead tried to numerically answer the question whether vortex sheets roll up.^[5] The first regularised vortex methods appeared much later in the early 1970s due to Chorin,^[6] who used a blob-based regularisation, and Christiansen,^[7] who used a grid-based regularisation on simple, rectangular domains. The underlying ideas of particle methods have been re-introduced in different contexts at least three times: in the late 1950s Harlow^[8] and Evans and Harlow^[9] introduced the Particle-in-Cell (PIC) method. The mapping between particle and grid quantities is a regularisation step, though this fact is not emphasised in these works. Lucy^[10] as well as Gingold and Monaghan^[11] laid the ground for Smoothed Particle Hydrodynamics (SPH), making use of a blob-based regularisation.

Vortex particle methods using the blob-regularisation were first analysed by Dushane^[12] and later by Hald and Mauceri Del Prete^[13] and Hald.^[14] Many contributions followed their work, and we refer to Leonard^{[15],[16]} for historic comments. Later it was realised that particle approximations that are interpreted as a quadrature rule correspond to *exact solutions* of a weak formulation of the transport equation. This led to a new, simplified type of convergence proofs due to Raviart^[2] and Cottet.^[17] To our knowledge, the latter work also contains the first convergence proofs for vortex methods using a grid-based regularisation. In the year 2000 Cottet and Koumoutsakos published the first monograph on vortex methods.^[3] This work also contains many more historic remarks and an extensive bibliography. Recently, we proposed regularisation schemes based on the L^2 -projection onto finite element and spline spaces with similar error bounds that also work in general, bounded domains.^{[18],[19]} These techniques are reminiscent of the earlier FEM-blobs suggested by Merriman.^[20] All of these analyses feature typical error-bounds like the one in equation (1).

In the context of vortex methods, remeshing was introduced by Koumoutsakos.^[21] It now is ubiquitous in practice,^{[22],[23],[24]} and has also been the subject of numerical analysis.^[25]

Cohen and Berthame^[26] pointed out that, at least in principle, the optimal convergence order $\mathcal{O}(\sigma^n)$ can be restored in particle methods when considering function values u_i instead of weights $w_i u_i$. They devise a scheme that employs discontinuous, piece-wise polynomial interpolations to achieve this error-bound. The triangulated vortex method of Russo and Strain^[27] creates a triangulation of the domain using the particle locations as grid-points. The particle field is then regularised by using piece-wise linear interpolation on each triangle.

The approach discussed in this article is slightly similar in the regard that it also uses function values u_i and a finite element function space. However it differs in the regard that it additionally makes use of the quadrature weights w_i , does not require a triangulation that follows the grid-points, and easily generalises to bounded domains and arbitrary order $n \in \mathbb{N}$. Moreover, our method is conservative.

4 Regularisation by Projection

Assume we are given a continuous finite element space $V_\sigma^n(\Omega) \subset C(\Omega)$ of mesh-width σ and order $n \in \mathbb{N}$. Furthermore assume that we are given a particle approximation $u_h = \sum_{i=1}^N w_i u_i \delta_{\mathbf{x}_i}$ that we want to regularise, where for brevity we sometimes omit the dependency on time t in our notation. Regularisation by projection now corresponds to finding the solution $u_{h,\sigma} \in V_\sigma^n(\Omega)$ of the following system:

$$\int_{\Omega} u_{h,\sigma} v_\sigma \, d\mathbf{x} = \sum_{i=1}^N w_i u_i v_\sigma(\mathbf{x}_i) \quad \forall v_\sigma \in V_\sigma^n(\Omega). \quad (10)$$

Together with a fictitious domain approach, this idea generalises to arbitrary domains Ω , and a numerical analysis^{[18],[19]} reveals error bounds of the type (1). The new approach consists of replacing the *exact integral* on the left by *numerical integration* using the nodes \mathbf{x}_i and weights w_i of u_h , i. e., we instead find $u_{h,\sigma} \in V_\sigma^n(\Omega)$ such that:

$$\sum_{i=1}^N w_i u_{h,\sigma}(\mathbf{x}_i) v_\sigma(\mathbf{x}_i) = \sum_{i=1}^N w_i u_i v_\sigma(\mathbf{x}_i) \quad \forall v_\sigma \in V_\sigma^n(\Omega). \quad (11)$$

Despite the additional error from discretising the integral, this approach does in fact yield the desired error-bound of $\mathcal{O}(\sigma^n)$ for $h \sim \sigma$ and arbitrary $m \geq 1$. The following three sub-sections are devoted to proving this claim. Afterwards we discuss the relationship of this method to conventional blob-based approaches.

4.1 Spline Spaces

For our ansatz spaces $V_\sigma^n(\Omega)$ we will use Cartesian tensor product splines, although other conventional, $W^{1,\infty}(\Omega)$ -conforming finite element spaces would also be possible. Let us create a Cartesian grid of size $\sigma > 0$ for the domain $\Omega = (0, 1)^D$, whose cubes we will refer to as $Q_i^\sigma \in \Omega$. For $n \in \mathbb{N}$ we then define our ansatz space as follows:

$$V_\sigma^n(\Omega) := \{u \in C^{n-2}(\Omega) : u|_{Q_i^\sigma} \in \mathbb{Q}_{n-1}, Q_i^\sigma \in \Omega\}, \quad (12)$$

where \mathbb{Q}_{n-1} refers to the space of polynomials of *coordinate-wise* degree $n - 1$ or less. For $n = 1$ one obtains the space of piecewise constants. To ensure continuity, we will later restrict ourselves to $n \geq 2$.

It will sometimes be useful to specify the norm we employ on these spaces explicitly. In these cases, for $p \in [1, \infty]$, we will write $V_\sigma^{n,p}(\Omega)$ to refer the space $V_\sigma^n(\Omega)$ equipped with the $L^p(\Omega)$ -norm. In the other cases the index p will be omitted. Furthermore, in analogy to the Sobolev Spaces, we will write $V_\sigma^{-n,p}(\Omega)$ for the normed dual of $V_\sigma^{n,q}(\Omega)$, $\frac{1}{p} + \frac{1}{q} = 1$.

We will assume that the reader is familiar with the basic properties of these spaces, which are, e. g., described in great detail Schumaker's book.^[28] We will in particular make use of the quasi-interpolator $P_\sigma^n : L^1(\Omega) \rightarrow V_\sigma^n(\Omega)$, which has the following properties:^[28, Theorems 12.6 and 12.7]

$$\|P_\sigma^n u\|_{W^{s,p}(Q_i^\sigma)} \lesssim \|u\|_{W^{s,p}(\hat{Q}_i^\sigma)} \quad \forall Q_i^\sigma \in \Omega, 0 \leq s \leq n - 1, p \in [1, \infty], \quad (13)$$

$$\|u - P_\sigma^n u\|_{L^p(Q_i^\sigma)} \lesssim \sigma^s |u|_{W^{s,p}(\hat{Q}_i^\sigma)} \quad \forall Q_i^\sigma \in \Omega, 0 \leq s \leq n, p \in [1, \infty], \quad (14)$$

where the hidden constants only depend on n, D , and s . Here $\hat{Q}_i^\sigma \supset Q_i^\sigma$ is only slightly larger than Q_i^σ , in particular we have $\text{meas}_D(\hat{Q}_i^\sigma) \leq C(n, D)\sigma^D$. $P_\sigma^n u$ also approximates the derivatives of u , but for simplicity we will only discuss the $L^p(\Omega)$ -norms here.

We will also make frequent use of so-called inverse estimates, which for $v \in V_\sigma^n(\Omega)$ allow us to estimate stronger norms by weaker ones.^[1, Section 4.5] For this let Q_i^σ denote an arbitrary cube from the Cartesian grid. One then has locally:

$$\|u\|_{W^{s,p}(Q_i^\sigma)} \lesssim \sigma^{\frac{D}{p} - \frac{D}{q}} \sigma^{r-s} \|u\|_{W^{r,q}(Q_i^\sigma)} \quad \forall p, q \in [1, \infty], 0 \leq r \leq s \leq n - 1, \quad (15)$$

and globally:

$$\|u\|_{W^{s,p}(\Omega)} \lesssim \sigma^{\min\{0, \frac{D}{p} - \frac{D}{q}\}} \sigma^{r-s} \|u\|_{W^{r,q}(\Omega)} \quad \forall p, q \in [1, \infty], 0 \leq r \leq s \leq n - 1. \quad (16)$$

Here the hidden constants only depend on p, q, n, r, s , and D . The global inequality holds in general for any finite union of entire cubes Q_i^σ from the Cartesian grid.

4.2 Particle Approximation

As mentioned before, for our purposes it is enough to consider quadrature rules of order $m = 1$. We create *another* Cartesian grid of size $h \leq \sigma$. Into each of its cells Q_i^h , $i = 1, \dots, N = h^{-D}$, we place a particle \mathbf{x}_i with weight $w_i := h^D$. The particles do not necessarily need to be placed at the centres. The particles are then moved over time according to $\dot{\mathbf{x}}_i(t) = \mathbf{a}(\mathbf{x}_i(t), t)$, $i = 1, \dots, N$. To fully specify the particle approximation $u_h(t) = \sum_{i=1}^N w_i u_i \delta_{\mathbf{x}_i(t)}$, we define $u_i = u_0(\mathbf{x}_i(0))$.

LEMMA 4.1. *Let $u_\sigma, v_\sigma \in V_\sigma^n(\Omega)$, $n \geq 2$, and $h \leq \sigma$. Then for all times $t \in [0, T]$ one has with the hidden constant depending on \mathbf{a} , n , D , and T :*

$$\left| \int_{\Omega} u_\sigma v_\sigma \, d\mathbf{x} - \sum_{i=1}^N w_i u_\sigma(\mathbf{x}_i(t)) v_\sigma(\mathbf{x}_i(t)) \right| \lesssim h |u_\sigma v_\sigma|_{W^{1,1}(\Omega)}. \quad (17)$$

Proof. Let us abbreviate $f := u_\sigma v_\sigma$, and note that because $n \geq 2$ we have $f \in W^{1,\infty}(\Omega)$. We furthermore denote $f_0 := f \circ \Phi_0^t$, $f_{0,h} := P_h^1 f_0$, and note that the quadrature rule integrates $f_{0,h} \circ \Phi_t^0$ exactly. Because $\nabla \cdot \mathbf{a} = 0$ we have $|\det \nabla \Phi_0^t| = |\det \nabla \Phi_t^0| = 1$.^[2, Lemma 1.2] We obtain by transforming the integral and (14):

$$\|f - f_{0,h} \circ \Phi_0^t\|_{L^1(\Omega)} = \|f \circ \Phi_0^t - f_{0,h}\|_{L^1(\Omega)} = \|f_0 - P_h^1 f_0\|_{L^1(\Omega)} \stackrel{(14)}{\lesssim} h |f_0|_{W^{1,1}(\Omega)}. \quad (18)$$

But because \mathbf{a} is smooth and bounded, so are the derivatives of Φ_0^t and we may write by Hölder's inequality $|f_0|_{W^{1,1}(\Omega)} = |f \circ \Phi_0^t|_{W^{1,1}(\Omega)} \lesssim |f|_{W^{1,1}(\Omega)}$. For the quadrature rule we obtain by the triangular inequality:

$$\sum_{i=1}^N w_i (f - f_{0,h} \circ \Phi_0^t)(\mathbf{x}_i(t)) \leq h^D \sum_{i=1}^N \|f - f_{0,h} \circ \Phi_0^t\|_{L^\infty(\Phi_0^t(Q_i^h))} = h^D \sum_{i=1}^N \|f_0 - f_{0,h}\|_{L^\infty(Q_i^h)}. \quad (19)$$

We now make use of the properties of P_h^1 and the boundedness of $\nabla \Phi_0^t$ to obtain:

$$h^D \sum_{i=1}^N \|f_0 - f_{0,h}\|_{L^\infty(Q_i^h)} \stackrel{(14)}{\lesssim} h^{1+D} \sum_{i=1}^N |f_0|_{W^{1,\infty}(\hat{Q}_i^h)} \lesssim h^{1+D} \sum_{i=1}^N |f|_{W^{1,\infty}(\Phi_0^t(\hat{Q}_i^h))}. \quad (20)$$

Because $|\det \nabla \Phi_0^t| = 1$ we have $\text{meas}_D(\Phi_0^t(\hat{Q}_i^h)) = \text{meas}_D(\hat{Q}_i^h) \lesssim h^D$. Furthermore, by the Lipschitz continuity of Φ_0^t , we obtain that $\text{diam}(\Phi_0^t(\hat{Q}_i^h)) \lesssim h$. For each index i there therefore exists a bounded number of cubes Q_j^σ whose union $K_i := \bigcup_j Q_j^\sigma$ covers $\Phi_0^t(\hat{Q}_i^h)$ and that fulfils $\text{meas}_D(K_i) \lesssim \sigma^D$. The K_i therefore cover Ω about $(\frac{\sigma}{h})^D$ times, and we thus obtain with together with inverse estimate (16):

$$\begin{aligned} h^{1+D} \sum_{i=1}^N |f|_{W^{1,\infty}(\Phi_0^t(\hat{Q}_i^h))} &\leq h^{1+D} \sum_{i=1}^N |f|_{W^{1,\infty}(K_i)} \stackrel{(16)}{\lesssim} h \left(\frac{h}{\sigma}\right)^D \sum_{i=1}^N |f|_{W^{1,1}(K_i)} \\ &\lesssim h \left(\frac{h}{\sigma}\right)^D \left(\frac{\sigma}{h}\right)^D |f|_{W^{1,1}(\Omega)} = h |f|_{W^{1,1}(\Omega)}. \end{aligned} \quad (21)$$

Thus we obtain in total:

$$\begin{aligned} \left| \int_{\Omega} u_\sigma v_\sigma \, d\mathbf{x} - \sum_{i=1}^N w_i u_\sigma(\mathbf{x}_i(t)) v_\sigma(\mathbf{x}_i(t)) \right| &= \\ \left| \int_{\Omega} f - f_{0,h} \circ \Phi_0^t \, d\mathbf{x} - \sum_{i=1}^N w_i (f - f_{0,h} \circ \Phi_0^t)(\mathbf{x}_i(t)) \right| &\lesssim h |u_\sigma v_\sigma|_{W^{1,1}(\Omega)}. \end{aligned} \quad (22) \quad \square$$

4.3 Convergence

Let $n \in \mathbb{N}$, $n \geq 2$, and $1 \leq p \leq \infty$. Given the quadrature rule from [subsection 4.2](#) at some time $t \in [0, T]$, we define the following operators:

$$A : V_\sigma^{n,p}(\Omega) \rightarrow V_\sigma^{-n,p}(\Omega), \quad \langle Au_\sigma, v_\sigma \rangle := \int_\Omega u_\sigma v_\sigma \, d\mathbf{x}, \quad (23)$$

$$A_h : V_\sigma^{n,p}(\Omega) \rightarrow V_\sigma^{-n,p}(\Omega), \quad \langle A_h u_\sigma, v_\sigma \rangle := \sum_{i=1}^N w_i u_\sigma(\mathbf{x}_i(t)) v_\sigma(\mathbf{x}_i(t)). \quad (24)$$

LEMMA 4.2 (STABILITY). *Let $h = d\sigma$, with $0 < d < 1$ independent of σ but small enough and $n \geq 2$. Then for all $t \in [0, T]$ the operator A_h is invertible and for all $1 \leq p \leq \infty$ its inverse is bounded:*

$$\|A_h^{-1}\|_{V_\sigma^{-n,p}(\Omega) \rightarrow V_\sigma^{n,p}(\Omega)} \leq C. \quad (25)$$

Proof. The proof for $p = 2$ is illustrative. Using the quadrature error estimate (17) and inverse inequality (16), one obtains that the operator A_h is coercive, i. e., for all $v_\sigma \in V_\sigma^n(\Omega)$ has:

$$\begin{aligned} \langle A_h v_\sigma, v_\sigma \rangle &= \langle A v_\sigma, v_\sigma \rangle - \langle (A - A_h) v_\sigma, v_\sigma \rangle \stackrel{(17)}{\geq} \|v_\sigma\|_{L^2(\Omega)}^2 - Ch |v_\sigma|_{W^{1,1}(\Omega)}^2 \\ &\stackrel{(16)}{\geq} \left(1 - \tilde{C} \frac{h}{\sigma}\right) \|v_\sigma\|_{L^2(\Omega)}^2 = (1 - \tilde{C}d) \|v_\sigma\|_{L^2(\Omega)}^2. \end{aligned} \quad (26)$$

For small enough d the operator A_h thus has an inverse that is bounded: $\|A_h^{-1}\|_{V_\sigma^{-n,2}(\Omega) \rightarrow V_\sigma^{n,2}(\Omega)} \leq C$. Note that \tilde{C} neither depends on h nor on σ , i. e., d can also be chosen independent of h and σ .

The exact operator A^{-1} is the $L^2(\Omega)$ -projector onto $V_\sigma^n(\Omega)$. Its boundedness for $1 \leq p \leq \infty$ has been shown by Douglas, Dupont, and Wahlbin,^[29] as well as Crouzeix and Thomée.^[30] The proof is technical, but with only minor modifications to account for the quadrature error directly carries over to A_h^{-1} . These modifications can be found in the appendix. Thus $\|A_h^{-1}\|_{V_\sigma^{-n,p}(\Omega) \rightarrow V_\sigma^{n,p}(\Omega)} \leq C$, $1 \leq p \leq \infty$. \square

As a direct corollary, one obtains that the system matrix corresponding to A_h in terms of the B-spline basis is not only sparse, but also symmetric positive definite and well-conditioned. Using the conjugate gradient method, the solution of (11) can thus be computed approximately at optimal time and space complexity $\mathcal{O}(N)$. This stability result will allow us to establish convergence. Because we take point evaluations of the initial data u_0 , it is most natural to consider the case $p = \infty$.

THEOREM 4.3 ($L^\infty(\Omega)$ -CONVERGENCE). *Let $u(\cdot, t)$, $t \in [0, T]$, denote the solution of the advection equation (2) with continuous initial data u_0 . Let $u_h(t)$ denote the particle approximation from [subsection 4.2](#). Then for $h = d\sigma$, with $0 < d < 1$ independent of σ but small enough, and $n \geq 2$ the following error-bound holds for the solution of (11), i. e., for $u_{h,\sigma}(\cdot, t) := A_h^{-1} u_h$:*

$$\|u_{h,\sigma}(\cdot, t) - u(\cdot, t)\|_{L^\infty(\Omega)} \lesssim \sigma^s \|u_0\|_{W^{s,\infty}(\Omega)} \quad 0 \leq s \leq n. \quad (27)$$

Proof. The key observation is the following. Let us for the moment assume that at the current time t the exact solution $u(\cdot, t)$ of the advection equation would be a spline: $u(\cdot, t) \in V_\sigma^n(\Omega)$. Noting that $u(\mathbf{x}_i(t), t) = u_i$ exactly, we immediately see that $u_{h,\sigma} := u(\cdot, t)$ solves (11). Because A_h is invertible, this is also the only solution, and in this case our approach yields the exact result.

In the general case we let $u_\sigma := P_\sigma^n u(\cdot, t)$ denote the quasi-interpolant of u onto $V_\sigma^n(\Omega)$. Furthermore, we set $(u_\sigma)_h := \sum_{i=1}^N w_i u_\sigma(\mathbf{x}_i(t)) \delta_{\mathbf{x}_i(t)}$ and obtain:

$$\begin{aligned} \|u_{h,\sigma} - u(\cdot, t)\|_{L^\infty(\Omega)} &= \|A_h^{-1} u_h - u\|_{L^\infty(\Omega)} \\ &\leq \|A_h^{-1} (u_h - (u_\sigma)_h)\|_{L^\infty(\Omega)} + \underbrace{\|A_h^{-1} (u_\sigma)_h - u_\sigma\|_{L^\infty(\Omega)}}_{=0} + \|u_\sigma - u(\cdot, t)\|_{L^\infty(\Omega)} \\ &\stackrel{(25)}{\lesssim} \|u_h - (u_\sigma)_h\|_{V_\sigma^{-n,\infty}(\Omega)} + \|u_\sigma - u(\cdot, t)\|_{L^\infty(\Omega)}. \end{aligned} \quad (28)$$

By (14), the last term can be bounded by $\sigma^s \|u(\cdot, t)\|_{W^{s,\infty}(\Omega)}$, and the stability of the advection equation (4) furthermore yields $\|u(\cdot, t)\|_{W^{s,\infty}(\Omega)} \lesssim \|u_0\|_{W^{s,\infty}(\Omega)}$.

It remains to show that we also have $\|u_h - (u_\sigma)_h\|_{V_\sigma^{-n,\infty}(\Omega)} \lesssim \sigma^s \|u_0\|_{W^{s,\infty}(\Omega)}$. Thus let $v_\sigma \in V_\sigma^n(\Omega)$ be arbitrary but fixed. Because we have $u_i = u(\mathbf{x}_i(t), t)$ exactly, one obtains:

$$\sum_{i=1}^N w_i (u_i - u_\sigma(\mathbf{x}_i(t))) v_\sigma(\mathbf{x}_i(t)) \leq \|u(\cdot, t) - u_\sigma\|_{L^\infty(\Omega)} \cdot \sum_{i=1}^N w_i \|v_\sigma\|_{L^\infty(\Phi_0^t(Q_i^h))}. \quad (29)$$

The sum can be bounded by $C\|v_\sigma\|_{L^1(\Omega)}$ using the same techniques as in the proof of Lemma 4.1, while for the first part we already established $\|u(\cdot, t) - u_\sigma\|_{L^\infty(\Omega)} \lesssim \sigma^s \|u_0\|_{W^{s,\infty}(\Omega)}$, and thus we in fact have $\|u_h - (u_\sigma)_h\|_{V_\sigma^{-n,\infty}(\Omega)} \lesssim \sigma^s \|u_0\|_{W^{s,\infty}(\Omega)}$ as desired. \square

In order to show convergence in $L^p(\Omega)$ for $p \neq \infty$, one requires inverse estimates. Let us thus consider the case where one initialises the particle approximation using $P_\sigma^{n+1}u_0$ instead of u_0 itself. For the initialisation we need to chose order $n+1$ as opposed to just n to ensure that we have $P_\sigma^{n+1}u_0 \in W^{n,\infty}(\Omega)$.

THEOREM 4.4 ($L^p(\Omega)$ -CONVERGENCE). *Let $u(\cdot, t)$, $t \in [0, T]$, denote the solution of the advection equation (2) with initial data $u_0 \in L^p(\Omega)$, $1 \leq p \leq \infty$. Let $u_h(t)$ denote the particle approximation from subsection 4.2, but with $u_i := (P_\sigma^{n+1}u_0)(\mathbf{x}_i(0))$, $i = 1, \dots, N$, $n \geq 2$. Then for $h = d\sigma$, with $0 < d < 1$ independent of σ but small enough the following error-bound holds for the solution of (11), i. e., for $u_{h,\sigma}(\cdot, t) := A_h^{-1}u_h$:*

$$\|u_{h,\sigma}(\cdot, t) - u(\cdot, t)\|_{L^p(\Omega)} \lesssim \sigma^s \|u_0\|_{W^{s,p}(\Omega)} \quad 0 \leq s \leq n, \quad p \in [1, \infty]. \quad (30)$$

Proof. Let $\tilde{u}(\cdot, t)$ denote the solution of the advection equation with u_0 replaced by $P_\sigma^{n+1}u_0$. We then have:

$$\|u(\cdot, t) - \tilde{u}(\cdot, t)\|_{L^p(\Omega)} \stackrel{(4)}{\lesssim} \|u_0 - P_\sigma^{n+1}u_0\|_{L^p(\Omega)} \stackrel{(14)}{\lesssim} \sigma^s \|u_0\|_{W^{s,p}(\Omega)} \quad 0 \leq s \leq n+1. \quad (31)$$

Therefore, the convergence order of the method does not deteriorate by replacing the initial data with its spline approximation. In complete analogy to the proof of Theorem 4.3, one obtains:

$$\|u_{h,\sigma} - \tilde{u}(\cdot, t)\|_{L^p(\Omega)} \lesssim \|u_h - (u_\sigma)_h\|_{V_\sigma^{-n,p}(\Omega)} + \|u_\sigma - \tilde{u}(\cdot, t)\|_{L^p(\Omega)}, \quad (32)$$

where the last term may be again bounded as desired:

$$\|u_\sigma - \tilde{u}(\cdot, t)\|_{L^p(\Omega)} \stackrel{(14)}{\lesssim} \sigma^s \|\tilde{u}(\cdot, t)\|_{W^{s,p}(\Omega)} \stackrel{(4)}{\lesssim} \sigma^s \|P_\sigma^{n+1}u_0\|_{W^{s,p}(\Omega)} \stackrel{(13)}{\lesssim} \sigma^s \|u_0\|_{W^{s,p}(\Omega)}, \quad 0 \leq s \leq n. \quad (33)$$

For the remaining term one obtains for arbitrary $v_\sigma \in V_\sigma^n(\Omega)$ using Hölder's inequality for $\frac{1}{p} + \frac{1}{q} = 1$ and the usual modifications for $p = \infty$ or $q = \infty$:

$$\sum_{i=1}^N w_i (u_i - u_\sigma(\mathbf{x}_i(t))) v_\sigma(\mathbf{x}_i(t)) \leq \left(\sum_{i=1}^N w_i \|\tilde{u}(\cdot, t) - u_\sigma\|_{L^\infty(\Phi_0^t(Q_i^h))}^p \right)^{\frac{1}{p}} \left(\sum_{i=1}^N w_i \|v_\sigma\|_{L^\infty(\Phi_0^t(Q_i^h))}^q \right)^{\frac{1}{q}}. \quad (34)$$

Now, using K_i from the proof of Lemma 4.1, the smoothness and boundedness of Φ_0^t and its inverse Φ_t^0 , the first sum may be bounded as follows:

$$\begin{aligned} \left(\sum_{i=1}^N w_i \|\tilde{u}(\cdot, t) - u_\sigma\|_{L^\infty(\Phi_0^t(Q_i^h))}^p \right)^{\frac{1}{p}} &\leq h^{\frac{D}{p}} \left(\sum_{i=1}^N \|\tilde{u}(\cdot, t) - u_\sigma\|_{L^\infty(K_i)}^p \right)^{\frac{1}{p}} \\ &\stackrel{(14)}{\lesssim} h^{\frac{D}{p}} \sigma^s \left(\sum_{i=1}^N \|\tilde{u}(\cdot, t)\|_{W^{s,\infty}(\hat{K}_i)}^p \right)^{\frac{1}{p}} \lesssim h^{\frac{D}{p}} \sigma^s \left(\sum_{i=1}^N \|P_\sigma^{n+1}u_0\|_{W^{s,\infty}(\Phi_t^0(\hat{K}_i))}^p \right)^{\frac{1}{p}}. \end{aligned} \quad (35)$$

Analogously to the K_i , we may find a bounded number of cubes Q_i^σ that covers $\Phi_t^0(\hat{K}_i)$, such that their union L_i fulfils $\text{meas}_D(L_i) \lesssim \sigma^D$. Moreover, the L_i cover Ω about $(\frac{\sigma}{h})^D$ times. Thus we obtain using inverse estimate (16):

$$\begin{aligned} h^{\frac{D}{p}} \sigma^s \left(\sum_{i=1}^N \|P_\sigma^{n+1} u_0\|_{W^{s,\infty}(\Phi_t^0(\hat{K}_i))}^p \right)^{\frac{1}{p}} &\leq h^{\frac{D}{p}} \sigma^s \left(\sum_{i=1}^N \|P_\sigma^{n+1} u_0\|_{W^{s,\infty}(L_i)}^p \right)^{\frac{1}{p}} \\ &\stackrel{(16)}{\lesssim} \left(\frac{h}{\sigma} \right)^{\frac{D}{p}} \sigma^s \left(\sum_{i=1}^N \|P_\sigma^{n+1} u_0\|_{W^{s,p}(L_i)}^p \right)^{\frac{1}{p}} \lesssim \left(\frac{h}{\sigma} \right)^{\frac{D}{p}} \left(\frac{\sigma}{h} \right)^{\frac{D}{p}} \sigma^s \|P_\sigma^{n+1} u_0\|_{W^{s,p}(\Omega)} \stackrel{(13)}{\lesssim} \sigma^s \|u_0\|_{W^{s,p}(\Omega)}. \end{aligned} \quad (36)$$

Similarly, we obtain:

$$\left(\sum_{i=1}^N w_i \|v_\sigma\|_{L^\infty(\Phi_0^t(Q_i^h))}^q \right)^{\frac{1}{q}} \lesssim \|v_\sigma\|_{L^q(\Omega)}, \quad (37)$$

and thus $\|u_h - (u_\sigma)_h\|_{V_\sigma^{-n,p}(\Omega)} \lesssim \sigma^s \|u_0\|_{W^{s,p}(\Omega)}$. \square

4.4 Relation to Blob-Methods

The regularisation by projection approach may be called a Particle-in-Cell scheme, because of the presence of an underlying grid. However, the approach also corresponds to a classic blob-based method with a specially chosen blob-function $\zeta_\sigma(\mathbf{x}, \mathbf{y})$. In fact, for each $\mathbf{y} \in \Omega$, let us define the functions $\zeta_\sigma(\cdot, \mathbf{y})$ as $A^{-1}\delta_{\mathbf{y}}$ and $\zeta_{h,\sigma}(\cdot, \mathbf{y}) := A_h^{-1}\delta_{\mathbf{y}}$. We then have $A^{-1}u_h = \sum_{i=1}^N w_i u_i \zeta_\sigma(\mathbf{x}, \mathbf{x}_i)$ and $A_h^{-1}u_h = \sum_{i=1}^N w_i u_i \zeta_{h,\sigma}(\mathbf{x}, \mathbf{x}_i)$, respectively.

The projection approaches are thus in fact blob-based methods. Both $\zeta_\sigma(\cdot, \mathbf{y})$ and $\zeta_{h,\sigma}(\cdot, \mathbf{y})$ are decaying at an exponential rate away from \mathbf{y} , just like conventional blob-functions. Moreover, ζ_σ fulfils the moment conditions:

$$\int_{\Omega} \zeta_\sigma(\mathbf{x}, \mathbf{y}) \mathbf{x}^\alpha \, d\mathbf{x} = \langle A A^{-1} \delta_{\mathbf{y}}, \mathbf{x}^\alpha \rangle = \mathbf{x}^\alpha|_{\mathbf{x}=\mathbf{y}} \quad \forall |\alpha| < n, \quad (38)$$

while $\zeta_{h,\sigma}$ fulfils *discrete moment conditions*:

$$\sum_{i=1}^N w_i \zeta_{h,\sigma}(\mathbf{x}_i, \mathbf{y}) \mathbf{x}_i^\alpha = \langle A_h A_h^{-1} \delta_{\mathbf{y}}, \mathbf{x}^\alpha \rangle = \mathbf{x}^\alpha|_{\mathbf{x}=\mathbf{y}} \quad \forall |\alpha| < n. \quad (39)$$

The fact that these special blob-functions exist means that other techniques developed for blob-based approaches can also be applied in the current setting. Let us for example consider viscous effects with viscosity $\nu > 0$. Interestingly, for $\zeta_{h,\sigma}$, both Fishelov's scheme^[31] and the method of particle strength exchange^[32] coincide and reduce to:

$$\begin{cases} \frac{d\mathbf{x}_i}{dt}(t) = \mathbf{a}(\mathbf{x}_i(t), t), \\ \frac{du_i}{dt}(t) = \nu \Delta u_{h,\sigma}(\mathbf{x}_i(t)), \end{cases} \quad i = 1, \dots, N. \quad (40)$$

5 Numerical Experiments

In this section we will consider four different types of numerical experiments with (vortex) particle methods. In the first example we consider a low order computation on a two-dimensional benchmark that has been used before to visualise the necessity of remeshing in classical particle methods.^[22] Our experiment will show that by using A_h^{-1} no remeshing is necessary.

The second experiment similarly is of graphical nature: we apply the particle method to the problem of interface tracking using a level-set function. This function evolves over time according to the linear advection equation and thus perfectly fits into the framework considered here. The results highlight the absence of numerical diffusion in the scheme.

For the third series of experiments we developed a solver for the two-dimensional domain $\Omega = (0, 1)^2$ with periodic boundary conditions. We perform high-order, long-term simulations of a quasi-steady, but highly instable flow. Due to its instability, this flow is notoriously hard to accurately reproduce in long-term simulations. We compare the vortex method to a state-of-the-art flow solver:^[33] an eighth order, exactly divergence-free, hybridised discontinuous Galerkin (HDG8) method. The results show the vortex method to be competitive.

Finally, the fourth series of experiments is a convergence study on a fully three-dimensional flow-problem: the Arnold–Beltrami–Childress (ABC) flow. Despite the additional vortex stretching term in three-dimensional space, the vortex method remained stable.

5.1 Graphical Demonstration

Koumoutsakos, Cottet, and Rossinelli^[22] describe the following benchmark case in two dimensions in order to illustrate the necessity of remeshing. Let us consider the two-dimensional, incompressible Euler equations in their vorticity formulation in the whole-space:

$$\frac{\partial \omega}{\partial t} + (\mathbf{u} \cdot \nabla) \omega = 0. \quad (41)$$

Here the advected quantity is the vorticity. Following the fluid mechanics convention, it is labelled ω instead of u , while the velocity is denoted by \mathbf{u} instead of \mathbf{a} . It is computed from ω via:

$$\psi(\mathbf{x}) := G \star \omega := \frac{1}{2\pi} \int_{\mathbb{R}^2} \ln \left(\frac{1}{|\mathbf{x} - \mathbf{y}|} \right) \omega(\mathbf{y}) \, \mathrm{d}\mathbf{y}, \quad (42)$$

$$\mathbf{u}(\mathbf{x}) := \operatorname{curl} \psi := \left(\frac{\partial \psi}{\partial x_2}(\mathbf{x}), -\frac{\partial \psi}{\partial x_1}(\mathbf{x}) \right)^\top. \quad (43)$$

A steady solution of this equation is given by:

$$\omega(\mathbf{x}, t) = 100 \max\{1 - 2|\mathbf{x}|, 0\}. \quad (44)$$

Note that the vorticity is compactly supported, while the velocity has global support. The streamlines corresponding to \mathbf{u} are concentric circles around the origin.

The task is now to construct a vortex particle method that reproduces this result over extended periods of time. We will artificially restrict ourselves to the domain $\Omega := (-1, 1)^2$, which contains the entire support of ω . Due to the circular motion particles will inevitably leave this domain. For this reason our particle field $\omega_h(0)$ will be created and tracked on the slightly larger domain $\Xi := (-2, 2)^2$ as described in [subsection 4.2](#). We will use $\sigma = 0.01$, $d = 0.5$, $h = 0.005$. At any time t , only the particles that are currently located inside of Ω will be considered for computing $\omega_{h,\sigma} := A_h^{-1} \omega_h \in V_\sigma^n(\Omega)$. We choose $n = 2$: it does not make sense to choose higher orders due to the low regularity of the exact solution.

In order to compute the velocity field, $\omega_{h,\sigma}$ is extended with zero outside of Ω and inserted into equation (42). The integral can be evaluated analytically: $\omega_{h,\sigma}$ is a piece-wise polynomial on a Cartesian grid. For a faster evaluation, however, we instead compute $\psi_{h,\sigma}$, the $L^2(\Xi)$ -projection of $G \star \omega_{h,\sigma}$ onto $V_\sigma^{n+2}(\Xi)$. The computation of this projection can be accelerated by a fast multipole method. The resulting function $\mathbf{u}_{h,\sigma} := \operatorname{curl} \psi_{h,\sigma}$ is supported on all of Ξ and by construction exactly divergence-free. It is used to convect *all particles*—also those outside of Ω —according to $\dot{\mathbf{x}}_i(t) = \mathbf{u}_{h,\sigma}(\mathbf{x}_i(t))$. These ODEs are discretised using the classical Runge–Kutta method and a fixed time-step of $\Delta t = 0.005$.

The results of this experiment are depicted in [Figure 1](#). In the first row the simulation was carried out with $A^{-1} u_h$ instead of $\omega_{h,\sigma} = A_h^{-1} \omega_h$. The first row clearly shows that the error quickly increases

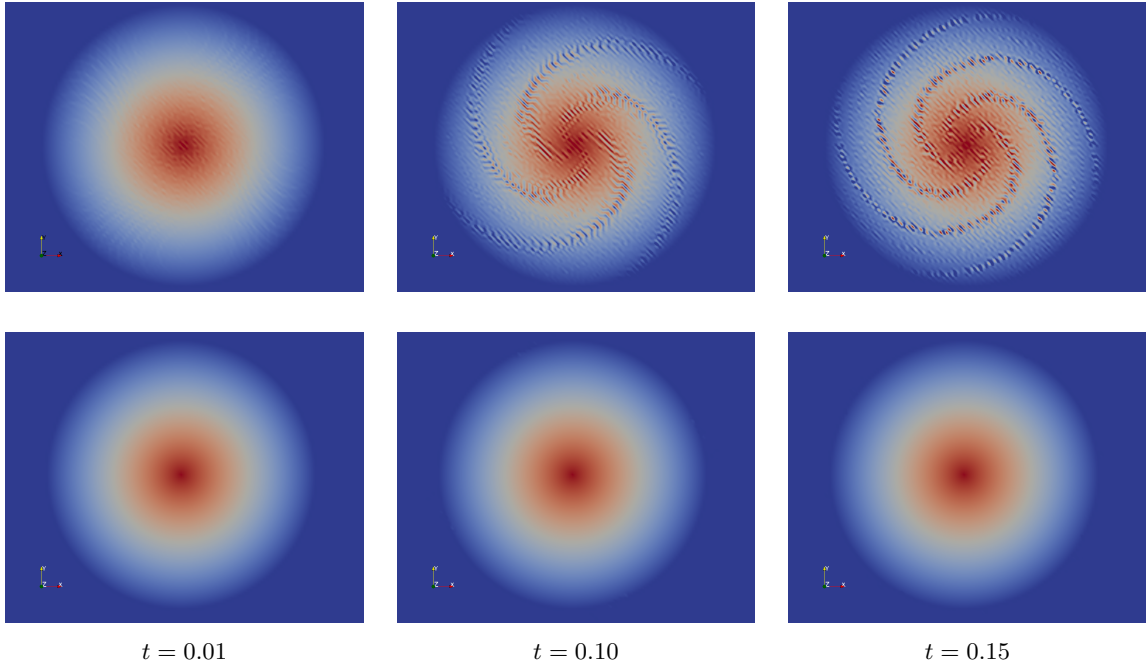


Figure 1: A comparison of $A^{-1}\omega_h$ in the first row and $A_h^{-1}\omega_h$ in the second. The first row corresponds to a classic vortex blob-method. Artefacts already appear in the beginning of the simulation and worsen over time. The second row shows the results of the new scheme which remain virtually unchanged over time as desired.

with time t . The reader is invited to compare this picture with those of Koumoutsakos, Cottet, and Rossinelli.^[22] On the other hand, the solution using $A_h^{-1}\omega_h$ remained accurate, despite the complete absence of any remeshing.

5.2 Application to Zalesak’s Disk

A great advantage of particle methods when applied to the advection equation is their complete lack of numerical diffusion. This makes them particularly interesting for interface tracking using the level-set method. A long established benchmark problem in the field is Zalesak’s disk, in which the evolution of a slitted disk subject to a rigid body rotation is tracked over time.^[34] The core difficulty here is to maintain the sharp kinks and corners of this domain: in many conventional schemes the corners quickly get smeared out.

We consider Zalesak’s disk on the domain $\Omega := [-0.5, 0.5]^2$ and the time interval $t \in [0, 628]$. The quantity of interest here is the signed distance function u , whose initial data u_0 is given as an algorithm in the appendix. This function evolves over time according to the advection equation (2) with a given velocity field. In this test-case we thus follow the notation of Section 2 and give the velocity field as:

$$\mathbf{a}(x, y) := \frac{2\pi}{628} \begin{pmatrix} -y \\ x \end{pmatrix}. \quad (45)$$

The discretisation is analogous to the previous subsection, with regularisation taking place on Ω , but particles being tracked on $\Xi := [-1, 1]^2 \supset \Omega$, with $n = 2$, $\sigma = 0.01$, $d = \frac{1}{2}$, $h = 0.005$, $\Delta t = 1$, where the classical Runge–Kutta method is used as a time-stepping scheme. The results together with the contour line of $u = 0$ are depicted in Figure 2. It can clearly be seen that the interface remains well-maintained, and does not degenerate over time. Due to the Lagrangian nature of the method, the results for $t = 0$ and $t = 628$ are identical, so this experiment can be extended to arbitrary time intervals.

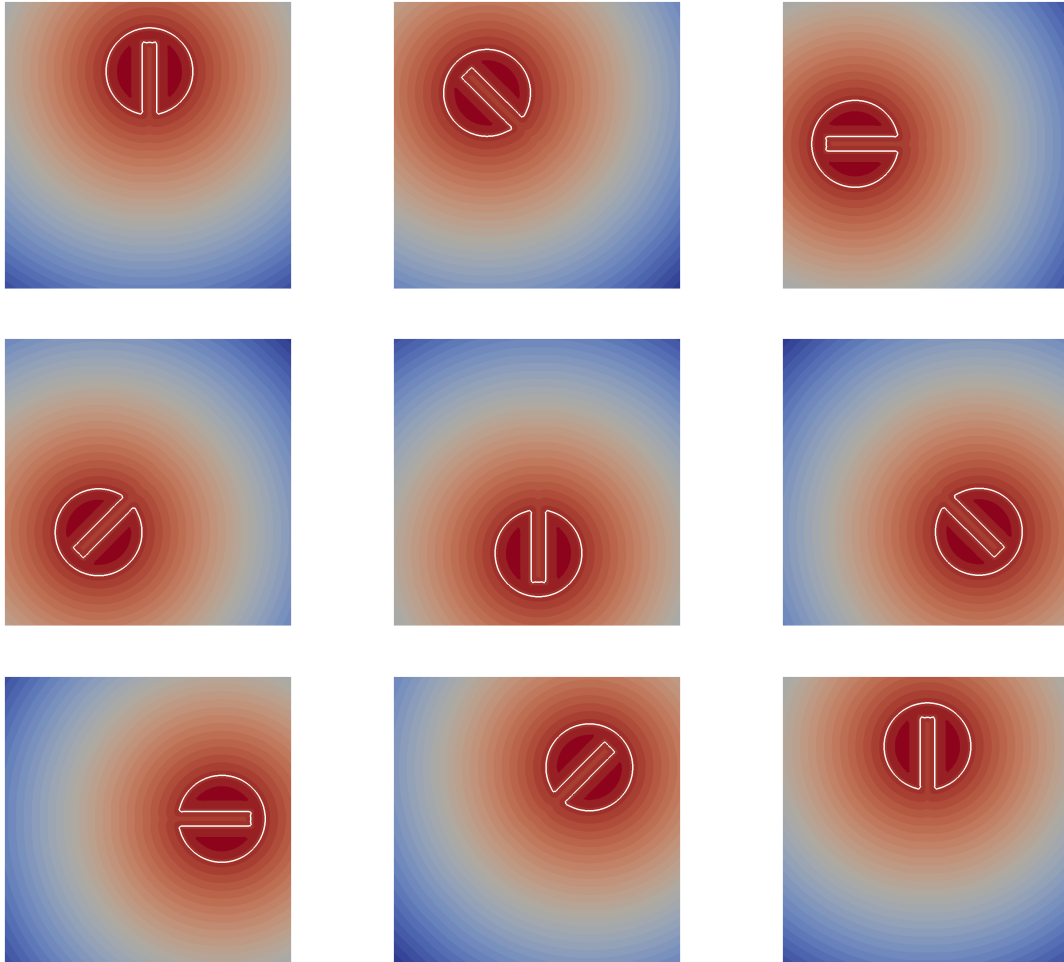


Figure 2: The signed-distance function and its zero contour for Zalesak's disk problem at times $t = 0, 79, 157, 236, 314, 393, 471, 550,$ and 628 . From left to right, top to bottom. There is no significant numerical diffusion: the corners do not get smeared out over time. Due to the Lagrangian nature of the method, the results for $t = 0$ and $t = 628$ are even identical.

5.3 Comparison with Discontinuous Galerkin Methods

Schroeder, Lehrenfeld, Linke, and Lube^[33] performed long-term simulations with $t \in [0, 26]$ of a two-dimensional flow on the domain $\Omega := (0, 1)^2$ with periodic boundary conditions. The exact solution to their benchmark problem reads:

$$\mathbf{u}_0(\mathbf{x}) = \begin{pmatrix} \sin(2\pi x_1) \sin(2\pi x_2) \\ \cos(2\pi x_1) \cos(2\pi x_2) \end{pmatrix}, \quad \mathbf{u}(\mathbf{x}, t) = e^{-8\pi^2 \nu t} \mathbf{u}_0(\mathbf{x}), \quad \nu = 10^{-5}. \quad (46)$$

This flow is dynamically unstable and small perturbations quickly lead to chaotic motion. In numerical methods this will inevitably occur, the challenge is to minimise the rate at which the numerical solutions diverge.

In their paper they emphasise the importance of *exactly enforcing* $\nabla \cdot \mathbf{u} = 0$ in numerical simulations. Methods that do not share this property, e. g., finite element formulations based on the Taylor–Hood pair, lose 12 significant digits before reaching $t = 2$. Schroeder, Lehrenfeld, Linke, and Lube applied an exactly divergence free, eighth order, hybridised discontinuous Galerkin formulation (HDG8) to this problem. In their simulation the rate of error increase was significantly smaller. Vortex methods also fulfil $\nabla \cdot \mathbf{u} = 0$ exactly, and we were kindly provided with the HDG8 simulation results for a comparison.

The two-dimensional Navier–Stokes equations in their vorticity formulation read:

$$\frac{\partial \omega}{\partial t} + (\mathbf{u} \cdot \nabla) \omega = \nu \Delta \omega. \quad (47)$$

Here, the velocity $\mathbf{u} = (u_1, u_2)^\top$ is the solution to the system:

$$\begin{cases} \partial_{x_1} u_1 + \partial_{x_2} u_2 = 0, \\ \partial_{x_1} u_2 - \partial_{x_2} u_1 = \omega. \end{cases} \quad (48)$$

The solution to this system can be obtained from ω by first solving the Poisson problem $-\Delta \psi = \omega$ for the stream function ψ with periodic boundary conditions and then setting $\mathbf{u} = (\partial_{x_2} \psi, -\partial_{x_1} \psi)^\top$ as before. The vortex particle method discretises this set of equations and proceeds in the following steps:

1. Let $t = 0$ and initialise the particle field ω_h from $\omega_0 = \text{curl } \mathbf{u}_0 = \partial_{x_1} u_{0,2} - \partial_{x_2} u_{0,1}$ as described in subsection 4.2. We place the particles at *random locations* inside the cells of the h -grid: the spectral accuracy of the mid-point rule in this case would give a wrong picture of the method's accuracy.
2. Repeat until $t = T$:
 - 2.1. Compute $\omega_{\sigma,h}(\cdot, t) = A_h^{-1} \omega_h(t)$ in $V_\sigma^n(\Omega)$, where the space $V_\sigma^n(\Omega)$ is supplemented with periodic boundary conditions.
 - 2.2. Solve the Poisson problem $-\Delta \psi_{\sigma,h}(\cdot, t) = \omega_{h,\sigma}(\cdot, t)$ in $V_\sigma^{n+2}(\Omega)$, again with periodic boundary conditions. We use a standard Galerkin method for this.
 - 2.3. Define $\mathbf{u}_{h,\sigma}(\cdot, t) := (\partial_{x_2} \psi_{h,\sigma}(\cdot, t), -\partial_{x_1} \psi_{h,\sigma}(\cdot, t))^\top$.
 - 2.4. Advance the following system of ODEs by one step Δt in time using, e. g., a Runge–Kutta method:

$$\begin{cases} \frac{d\mathbf{x}_i}{dt}(t) = \mathbf{u}_{h,\sigma}(\mathbf{x}_i(t), t), \\ \frac{d\omega_i}{dt}(t) = \nu \Delta \omega_{h,\sigma}(\mathbf{x}_i(t), t), \end{cases} \quad i = 1, \dots, N. \quad (49)$$

Schroeder, Lehrenfeld, Linke, and Lube^[33] performed their simulations on unstructured grids of sizes $\sigma \approx 0.25$ and $\sigma \approx 0.05$, together with a second order time discretisation and a fixed time-step of $\Delta t = 10^{-4}$. We perform our experiments with $\sigma \in \{\frac{1}{13}, \frac{1}{30}\}$, $h = \frac{\sigma}{2}$, i. e., $d = \frac{1}{2}$, and orders $n \in \{4, 6, 8\}$. The grid-sizes were chosen such that for $\sigma = \frac{1}{13}$ the initial $L^2(\Omega)$ -error in the velocity for $n = 6$ roughly

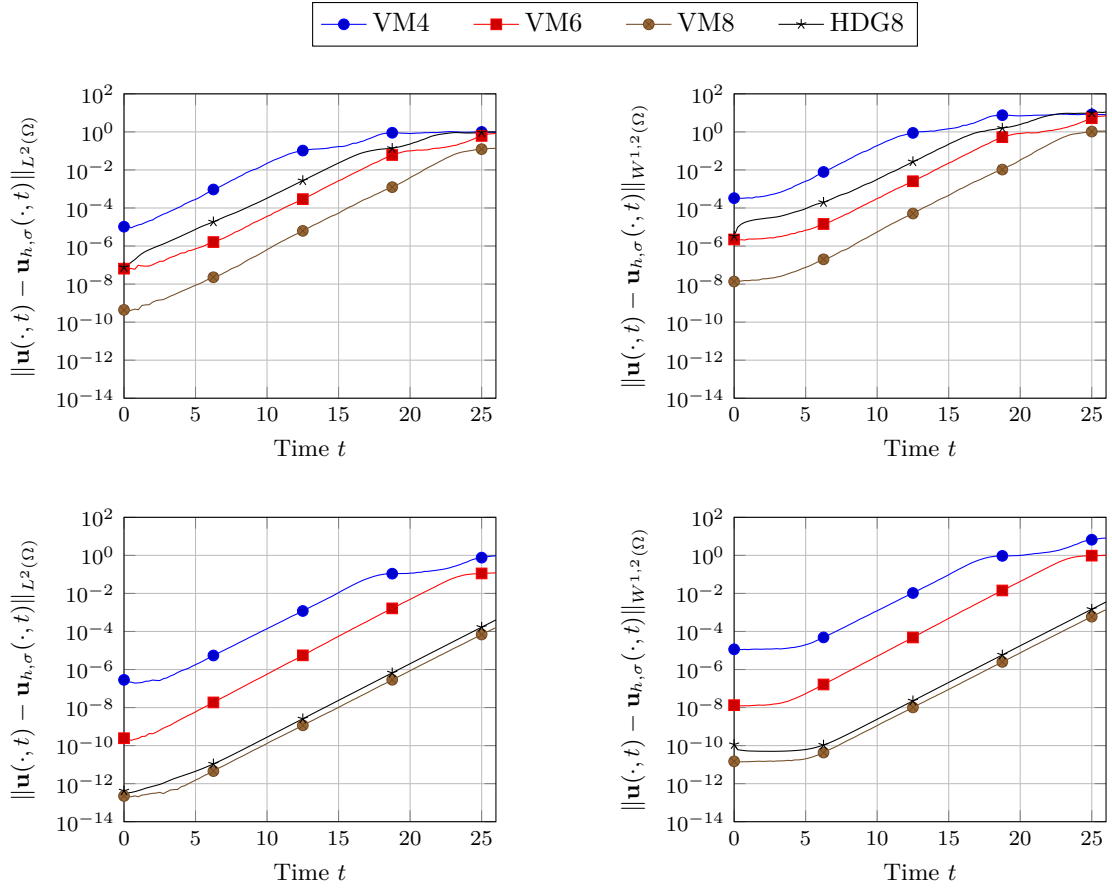


Figure 3: Evolution of the $L^2(\Omega)$ - and $W^{1,2}(\Omega)$ -errors of the fourth, sixth, and eighth order vortex methods over time in comparison to an eighth order discontinuous Galerkin scheme on coarse (top) and fine (bottom) meshes.

equals that of the HDG8 computation on the coarse mesh. Similarly, for $\sigma = \frac{1}{30}$ the initial error of the HDG8 scheme roughly equals that of the eighth order vortex method. For the time discretisation we use Verner's 'most efficient' ninth order Runge–Kutta method^[35] with a fixed time-step of $\Delta t = \frac{1}{32}$. This time-step is more than 300 times larger than the one used for the HDG8 computations.

The results are depicted in Figure 3. One clearly sees that the vortex methods perform very much like the HDG8 schemes and that errors increase at an equal rate. We conclude that vortex methods can compete with state-of-the-art discontinuous Galerkin methods. At the same time, due to the high degree of regularity of the ansatz spaces, very few degrees of freedom (DOF) are necessary. In fact, in this particular case we have three degrees of freedom per particle (two for \mathbf{x}_i and one for ω_i) and two per grid-node (one each for $\psi_{h,\sigma}$ and $\omega_{h,\sigma}$); both numbers are independent of the order n . For $\sigma = \frac{1}{30}$ one obtains $N_{\text{DOF}} = 2 \times 30^2 + 3 \times 60^2 = 12\,600$ compared to 23 903 non-eliminable DOFs for the HDG8 scheme.

5.4 Application to a three-dimensional Flow

As an example of a three-dimensional problem, we consider the Arnold–Beltrami–Childress flow [36, pp. 56ff] on the domain $\Omega = (0, 2\pi)^3$ for $t \in [0, 10]$:

$$\mathbf{u}_0(\mathbf{x}) = \begin{pmatrix} \sin(x_3) + \cos(x_2) \\ \sin(x_1) + \cos(x_3) \\ \sin(x_2) + \cos(x_1) \end{pmatrix}, \quad \mathbf{u}(\mathbf{x}, t) = e^{-\nu t} \mathbf{u}_0(\mathbf{x}), \quad \nu = 10^{-3}. \quad (50)$$

This flow is one of the few known fully three-dimensional, analytic solutions to the Navier–Stokes equations with periodic boundary conditions. Due to the larger viscosity, this flow is only mildly unstable.

In three dimensional space, the vorticity formulation of the Navier–Stokes equations reads:

$$\frac{\partial \boldsymbol{\omega}}{\partial t} + (\mathbf{u} \cdot \nabla) \boldsymbol{\omega} = (\nabla \mathbf{u}) \cdot \boldsymbol{\omega} + \nu \Delta \boldsymbol{\omega}. \quad (51)$$

Unlike in two dimensions, the vorticity $\boldsymbol{\omega}$ now also is a vector-valued quantity, and the equation is augmented with the so-called *vortex stretching* term $(\nabla \mathbf{u}) \cdot \boldsymbol{\omega}$. The velocity \mathbf{u} can be obtained from the vorticity $\boldsymbol{\omega}$ by solving the system $\nabla \cdot \mathbf{u} = 0$, $\nabla \times \mathbf{u} = \boldsymbol{\omega}$. The vortex method discretises this set of equations analogously to the two-dimensional case:

1. Let $t = 0$ and initialise the particle field $\boldsymbol{\omega}_h$ from $\boldsymbol{\omega}_0 = \nabla \times \mathbf{u}_0$. We place the particles at *random locations* inside the cells of the h -grid.
2. Repeat until $t = T$:
 - 2.1. Compute $\boldsymbol{\omega}_{\sigma,h}(\cdot, t) = A_h^{-1} \boldsymbol{\omega}_h(t)$ in $(V_\sigma^n(\Omega))^3$, where the space $(V_\sigma^n(\Omega))^3$ is supplemented with periodic boundary conditions.
 - 2.2. Solve the Poisson problem $-\Delta \psi_{\sigma,h}(\cdot, t) = \boldsymbol{\omega}_{h,\sigma}(\cdot, t)$ in $(V_\sigma^{n+2}(\Omega))^3$, again with periodic boundary conditions. We use a standard Galerkin method for this.
 - 2.3. Define $\mathbf{u}_{h,\sigma}(\cdot, t) := \nabla \times \psi_{h,\sigma}(\cdot, t)$.
 - 2.4. Advance the following system of ODEs by one step Δt in time using, e. g., a Runge–Kutta method:

$$\begin{cases} \frac{d\mathbf{x}_i}{dt}(t) = \mathbf{u}_{h,\sigma}(\mathbf{x}_i(t), t), \\ \frac{d\boldsymbol{\omega}_i}{dt}(t) = \left[(\nabla \mathbf{u}_{h,\sigma}) \cdot (\nabla \times \mathbf{u}_{h,\sigma}) \right] (\mathbf{x}_i(t), t) + \nu \Delta \boldsymbol{\omega}_{h,\sigma}(\mathbf{x}_i(t), t), \end{cases} \quad i = 1, \dots, N. \quad (52)$$

We perform a convergence study using $\sigma \in [\frac{2\pi}{10}, \frac{2\pi}{40}]$, $h = \frac{\sigma}{2}$, i. e., $d = \frac{1}{2}$, $n \in \{4, 6\}$, and a fixed time-step of $\Delta t = \frac{1}{25}$ using Verner’s ninth order Runge–Kutta method.

For $\sigma = \frac{2\pi}{10}$ and $n = 4$ a video of the evolving particle field at 25 steps-per-second was created.* The reader is invited to take a look: while it is hard to measure the beauty of a method or flow, one can clearly see that this flow is non-trivial and that the particle method remains stable. This is also quantitatively confirmed in Figure 4, where the evolution of the $W^{1,2}(\Omega)$ velocity error over time is shown: while for the coarse discretisations the error grows only mildly over time, it stays essentially constant for the fine ones. In Table 1 the errors for the various discretisations at final time $T = 10$ are shown. The results confirm that the methods are of order n .

*<https://rwth-aachen.sciebo.de/s/5tueQcMJeqWjPut>, a temporary link for the preprint. Can be played using, e. g., the VLC Media Player.

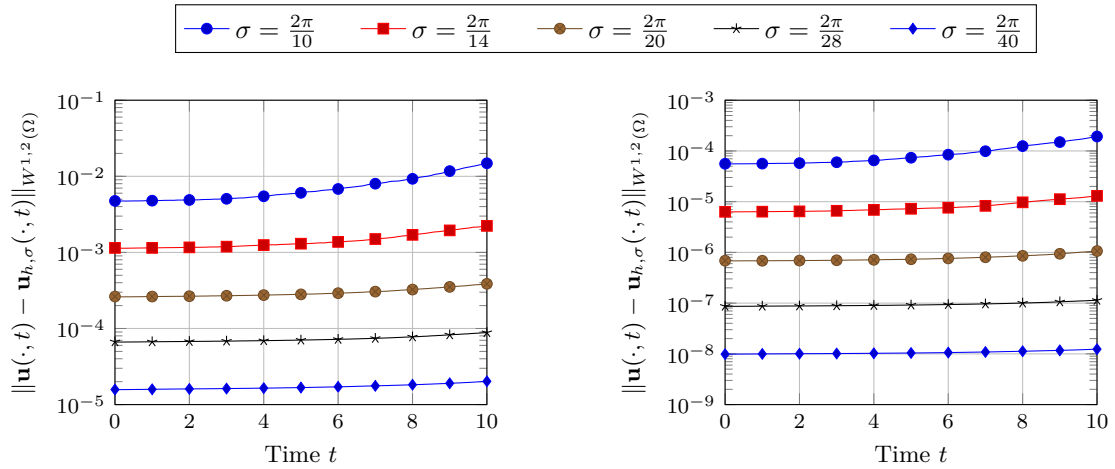


Figure 4: The evolution of the $W^{1,2}(\Omega)$ velocity error for the ABC flow problem. Note the different scales for order $n = 4$ on the left and order $n = 6$ on the right. The error increases only mildly over time for the coarse discretisations and stays almost unchanged for the fine ones.

$n = 4.$	$\ \mathbf{u} - \mathbf{u}_{h,\sigma}\ _{L^2(\Omega)}$	EOC	$\ \mathbf{u} - \mathbf{u}_{h,\sigma}\ _{W^{1,2}(\Omega)}$	EOC
$\sigma = \frac{2\pi}{10}$	3.60×10^{-3}	—	1.48×10^{-2}	—
$\sigma = \frac{2\pi}{14}$	4.12×10^{-4}	6.44	2.23×10^{-3}	5.62
$\sigma = \frac{2\pi}{20}$	5.17×10^{-5}	5.82	3.86×10^{-4}	4.92
$\sigma = \frac{2\pi}{28}$	1.01×10^{-5}	4.85	8.84×10^{-5}	4.38
$\sigma = \frac{2\pi}{40}$	2.45×10^{-6}	3.97	2.02×10^{-5}	4.14

$n = 6.$	$\ \mathbf{u} - \mathbf{u}_{h,\sigma}\ _{L^2(\Omega)}$	EOC	$\ \mathbf{u} - \mathbf{u}_{h,\sigma}\ _{W^{1,2}(\Omega)}$	EOC
$\sigma = \frac{2\pi}{10}$	4.63×10^{-5}	—	1.93×10^{-4}	—
$\sigma = \frac{2\pi}{14}$	2.44×10^{-6}	8.75	1.30×10^{-5}	8.02
$\sigma = \frac{2\pi}{20}$	1.36×10^{-7}	8.10	1.06×10^{-6}	7.03
$\sigma = \frac{2\pi}{28}$	1.12×10^{-8}	7.42	1.14×10^{-7}	6.63
$\sigma = \frac{2\pi}{40}$	1.30×10^{-9}	6.04	1.24×10^{-8}	6.22

Table 1: The $L^2(\Omega)$ and $W^{1,2}(\Omega)$ velocity errors at time $T = 10$ for the ABC flow problem at different discretisation sizes σ and orders $n = 4$ (top) and $n = 6$ (bottom). The empirical orders of convergence (EOC) approach the theoretical ones.

6 Outlook

The regularisation scheme considered in this article uses a uniform, non-adaptive Cartesian grid. As shown in theory and practice, this scheme is asymptotically optimal for convection dominated flows if both the initial data and the velocity field are sufficiently smooth. In these cases vortex methods in particular can compete with discontinuous Galerkin methods.

Many flows of practical interest, however, feature steep gradients, leading to similarly steep gradients in the solution. This is especially true for turbulent flows. If applied to such flows, the uniform regularisation scheme presented in this work requires very small choices of d for A_h^{-1} to remain well-conditioned, thereby reducing its efficiency.

The particles naturally adapt to such flow fields. In fact, particles cluster where steep gradients occur, while the particle field ‘thins out’ in the areas where gradients get flat. To see this, let us reconsider the analytic solution of the linear advection equation: $u(\mathbf{x}, t) = u_0(\Phi_t^0(\mathbf{x}))$. A simple application of the chain rule yields:

$$\nabla u(\mathbf{x}, t) = \nabla u_0(\Phi_t^0(\mathbf{x})) \cdot \nabla \Phi_t^0(\mathbf{x}). \quad (53)$$

Therefore, steep gradients that were not already present in u_0 can only arise if $\nabla \Phi_t^0$ is ‘large’. Let \mathbf{x}_i and \mathbf{x}_j denote two particles that are close to one another at time t and let $\mathbf{z} := (\mathbf{x}_j(t) - \mathbf{x}_i(t))/|\mathbf{x}_j(t) - \mathbf{x}_i(t)|$. We then have approximately:

$$\frac{\partial \Phi_t^0}{\partial \mathbf{z}}(\mathbf{x}_i(t)) \approx \frac{\Phi_t^0(\mathbf{x}_j(t)) - \Phi_t^0(\mathbf{x}_i(t))}{|\mathbf{x}_j(t) - \mathbf{x}_i(t)|} = \frac{\mathbf{x}_j(0) - \mathbf{x}_i(0)}{|\mathbf{x}_j(t) - \mathbf{x}_i(t)|}. \quad (54)$$

Thus, derivatives of Φ_t^0 get large when particles are close together that previously were not. Conversely, the derivatives are small if particles move away from one another. It therefore would make sense to also adapt the Ansatz spaces for the regularisation scheme accordingly: the resolution should be coarse where there are few particles and fine where there are many. This would also ensure that the operator A_h^{-1} corresponding to these spaces remains well-defined. In the context of splines it would be interesting to develop methods based on wavelets to achieve this adaption of the Ansatz spaces.

One can also assign new quadrature weights to a given particle field. For this one subdivides the domain Ω into new cells Q_i , such that each contains exactly one particle. Afterwards, each particle is assigned the weight $w_i = \text{meas}_{\mathbb{D}}(Q_i)$. We believe that this also makes our method interesting for scattered data approximation.

Another topic that was not covered in detail here is time discretisation. In this work we simply used standard Runge–Kutta methods. Given the apparent importance of exactly enforcing $\nabla \cdot \mathbf{u} = 0$ when solving the incompressible Navier–Stokes equations, it would make sense to use volume preserving schemes for solving the ODEs $\dot{\mathbf{x}}_i(t) = \mathbf{u}(\mathbf{x}_i(t), t)$, $i = 1, \dots, N$. Maybe this would even further improve the long-term accuracy of particle approximations when applied to such problems.

Appendix

Modification of the original Proof of $L^\infty(\Omega)$ -Stability^{[29],[30]}

To establish the boundedness of A_h^{-1} as an operator $V_\sigma^{-n,p}(\Omega) \rightarrow V_\sigma^{n,p}(\Omega)$, $p \neq 2$, it suffices to consider functionals of the form $\int_\Omega f v_\sigma dx$, $f \in L^p(\Omega)$. We thus let $f \in L^p(\Omega)$, fix a cell $Q_j^\sigma \in \Omega$ and define $f_j := f$ on Q_j^σ and $f_j := 0$ on $\Omega \setminus Q_j^\sigma$. We will establish that $f_{j,\sigma} := A_h^{-1} f_j$ decays at an exponential rate away from Q_j^σ .

We have for all $v_\sigma \in V_\sigma^n(\Omega)$ that vanish on Q_j^σ : $\langle A_h f_{j,\sigma}, v_\sigma \rangle = \int_{Q_j^\sigma} f v_\sigma dx = 0$. We now construct such a function v_σ . Let us define the neighbourhoods of Q_j^σ as $D_{j,0} := \emptyset$, $D_{j,1} := Q_j^\sigma$, and for all other $k \in \mathbb{N}$:

$$D_{j,k} := \bigcup \{Q_l^\sigma \in \Omega : |\text{centre}(Q_l^\sigma) - \text{centre}(Q_j^\sigma)|_\infty < k\sigma\}, \quad (55)$$

where $|\cdot|_\infty$ denotes the Manhattan distance norm on \mathbb{R}^D . We define v_σ as follows: for $k \geq n$ we let $v_\sigma = f_{j,\sigma}$ on $\Omega \setminus D_{j,k}$ and set the remaining B-spline coefficients to zero. It follows that $v_\sigma = 0$ on $D_{j,k-(n-1)}$. Thus, denoting the quadrature error $e := \sum_{i=1}^N w_i f_{j,\sigma}(\mathbf{x}_i) v_\sigma(\mathbf{x}_i) - \int_\Omega f_{j,\sigma} v_\sigma \, d\mathbf{x}$, we have:

$$\begin{aligned} 0 &= \sum_{i=1}^N w_i f_{j,\sigma}(\mathbf{x}_i) v_\sigma(\mathbf{x}_i) = \int_\Omega f_{j,\sigma} v_\sigma \, d\mathbf{x} + \left(\sum_{i=1}^N w_i f_{j,\sigma}(\mathbf{x}_i) v_\sigma(\mathbf{x}_i) - \int_\Omega f_{j,\sigma} v_\sigma \, d\mathbf{x} \right) \\ &\iff \int_{\Omega \setminus D_{j,k}} f_{j,\sigma} v_\sigma \, d\mathbf{x} + e = \int_{D_{j,k} \setminus D_{j,k-(n-1)}} f_{j,\sigma} v_\sigma \, d\mathbf{x} \\ &\iff \int_{\Omega \setminus D_{j,k}} f_{j,\sigma}^2 \, d\mathbf{x} + e = \int_{D_{j,k} \setminus D_{j,k-(n-1)}} f_{j,\sigma} v_\sigma \, d\mathbf{x}. \end{aligned} \quad (56)$$

Due to the stability of the B-spline basis, we have $\|v_\sigma\|_{L^2(D_{j,k} \setminus D_{j,k-(n-1)})} \leq C_1 \|f_{j,\sigma}\|_{L^2(D_{j,k} \setminus D_{j,k-(n-1)})}$. The right hand side of the last equation can thus be bounded from above by $C_1 \|f_{j,\sigma}\|_{L^2(D_{j,k} \setminus D_{j,k-(n-1)})}^2$. On the left we insert the quadrature error bound (17) with error constant C_2 and obtain:

$$\begin{aligned} \|f_{j,\sigma}\|_{L^2(\Omega \setminus D_{j,k})}^2 - C_2 h |f_{j,\sigma} v_\sigma|_{W^{1,1}(\Omega)} &\leq C_1 \|f_{j,\sigma}\|_{L^2(D_{j,k} \setminus D_{j,k-(n-1)})}^2 \\ &\iff \|f_{j,\sigma}\|_{L^2(\Omega \setminus D_{j,k})}^2 - C_2 h |f_{j,\sigma}^2|_{W^{1,1}(\Omega \setminus D_{j,k})} \leq \\ &\quad C_1 \|f_{j,\sigma}\|_{L^2(D_{j,k} \setminus D_{j,k-(n-1)})}^2 + C_2 h |f_{j,\sigma} v_\sigma|_{W^{1,1}(D_{j,k} \setminus D_{j,k-(n-1)})}. \end{aligned} \quad (57)$$

Now, using an inverse inequality, with constant C_3 :

$$C_2 h |f_{j,\sigma}^2|_{W^{1,1}(\Omega \setminus D_{j,k})} \leq C_2 C_3 \frac{h}{\sigma} \|f_{j,\sigma}\|_{L^1(\Omega \setminus D_{j,k})} = d C_2 C_3 \|f_{j,\sigma}\|_{L^2(\Omega \setminus D_{j,k})}^2. \quad (58)$$

The left side of the last inequality in (57) can thus be bounded from below by $C_4 \|f_{j,\sigma}\|_{L^2(\Omega \setminus D_{j,k})}^2$, with $C_4 = (1 - d C_2 C_3)$. For d small enough we have $C_4 > 0$. Similarly, the right side can be bounded by $C_5 \|f_{j,\sigma}\|_{L^2(D_{j,k} \setminus D_{j,k-(n-1)})}^2$, with error constant $C_5 = C_1(1 + d C_2 C_3)$. Thus, with $C_6 = \frac{C_5}{C_4}$:

$$\|f_{j,\sigma}\|_{L^2(\Omega \setminus D_{j,k})}^2 \leq C_6 \|f_{j,\sigma}\|_{L^2(D_{j,k} \setminus D_{j,k-(n-1)})}^2. \quad (59)$$

But we have $D_{j,k} \setminus D_{j,k-(n-1)} = (\Omega \setminus D_{j,k-(n-1)}) \setminus (\Omega \setminus D_{j,k})$, and thus we obtain:

$$\|f_{j,\sigma}\|_{L^2(\Omega \setminus D_{j,k})}^2 \leq \underbrace{\frac{C_6}{1 + C_6}}_{=: C_7} \|f_{j,\sigma}\|_{L^2(\Omega \setminus D_{j,k-(n-1)})}^2, \quad (60)$$

where we obviously have $0 < C_7 < 1$. For large values of k this argument can now now be repeated on the right hand side, and we obtain:

$$\|f_{j,\sigma}\|_{L^2(\Omega \setminus D_{j,k})}^2 \leq C_7^{\lfloor \frac{k}{n} \rfloor} \|f_{j,\sigma}\|_{L^2(\Omega)}. \quad (61)$$

This is the desired exponential decay. From here the proof is identical to the original ones.^{[29],[30]}

Source Code for the Initial Data of Zalesak's Disk

```
//
// Signed distance function for Zalesak's disk.
//
real initial_data( point x )
{
    using std::min;
```

```

constexpr point A { 0, 0, 0 };
constexpr point B { 0, 0.25, 0 };
constexpr point C { -0.025, 0.35, 0 };
constexpr point D { 0.025, 0.35, 0 };
constexpr real R { 0.15 };
const real phi { std::asin(0.025/0.15) };
constexpr point E { -0.025, 0.25 - R*std::cos(phi), 0 };
constexpr point F { 0.025, 0.25 - R*std::cos(phi), 0 };

auto is_in_cone = [phi]( point x ) noexcept -> bool
{
    return std::acos( scal_prod(x-B,A-B)/((x-B).r() * (A-B).r() ) ) < phi;
};

auto is_in_box = [C,D]( point x ) noexcept -> bool
{
    return (x.x > C.x) && (x.x < D.x) && (x.y < D.y);
};

if ( length(x-B)<R )
{
    if ( is_in_box(x) )
    {
        if ( x.y < F.y )
        {
            return -min(length(x-E),length(x-F));
        }
        else
        {
            return -min( min(x.x-E.x,F.x-x.x), C.y-x.y );
        }
    }
    else
    {
        if ( x.y > D.y )
        {
            real dist = min( min(length(x-C),length(x-D)), R-length(x-B) );
            if ( C.x < x.x && x.x < D.x ) return min(dist,x.y-C.y);
            else return dist;
        }
        else
        {
            if ( x.x < B.x )
            {
                return min( C.x - x.x, R - length(x-B) );
            }
            else
            {
                return min( x.x - D.x, R - length(x-B) );
            }
        }
    }
}
else
{
    if ( is_in_cone(x) )

```

```

    {
        return -std::min(length(x-E), length(x-F));
    }
    else
    {
        return -((x-B).r() - R);
    }
}
}

```

References

- [1] S. C. Brenner and L. R. Scott. *The Mathematical Theory of Finite Element Methods*. 3rd ed. Vol. 15. Texts in Applied Mathematics. Springer, 2008. ISBN: 9780387759333. DOI: [10.1007/978-0-387-75934-0](https://doi.org/10.1007/978-0-387-75934-0).
- [2] P.-A. Raviart. ‘An Analysis of Particle Methods’. In: *Numerical Methods in Fluid Dynamics*. Ed. by F. Brezzi. Vol. 1127. Lecture Notes in Mathematics. Springer, 1984. Chap. 4, pp. 243–324. ISBN: 9783540152255. DOI: [10.1007/BFb0074532](https://doi.org/10.1007/BFb0074532).
- [3] G.-H. Cottet and P. D. Koumoutsakos. *Vortex Methods. Theory and Practice*. Cambridge University Press, 2000. ISBN: 0521621860. DOI: [10.1017/CB09780511526442](https://doi.org/10.1017/CB09780511526442).
- [4] S. L. Sobolev and V. L. Vaskevich. *The Theory of Cubature Formulas*. Trans. by S. S. Kutateladze. 1st ed. Mathematics and Its Applications 415. Springer, 1997. ISBN: 9789048148752. DOI: [10.1007/978-94-015-8913-0](https://doi.org/10.1007/978-94-015-8913-0).
- [5] L. Rosenhead. ‘The Formation of Vortices from a Surface of Discontinuity’. In: *Proceedings of the Royal Society of London* 142.832 (Nov. 1931), pp. 170–192.
- [6] A. J. Chorin. ‘Numerical study of slightly viscous flow’. In: *Journal of Fluid Mechanics* 57.4 (Mar. 1973), pp. 785–796. ISSN: 0022–1120. DOI: [10.1017/S0022112073002016](https://doi.org/10.1017/S0022112073002016).
- [7] J. P. Christiansen. ‘Numerical Simulation of Hydrodynamics by the Method of Point Vortices’. In: *Journal of Computational Physics* 13.3 (Nov. 1973), pp. 363–379. ISSN: 0021–9991. DOI: [10.1016/0021-9991\(73\)90042-9](https://doi.org/10.1016/0021-9991(73)90042-9).
- [8] F. H. Harlow. ‘Hydrodynamic Problems Involving Large Fluid Distortions’. In: *Journal of the Association of Computing Machinery* 4.2 (Apr. 1957), pp. 137–142. ISSN: 0004–5411. DOI: [10.1145/320868.320871](https://doi.org/10.1145/320868.320871).
- [9] M. W. Evans and F. H. Harlow. *The Particle-in-Cell Method for Hydrodynamic Calculations*. Report LA-2139. Los Alamos Scientific Laboratory of the University of California, 1957.
- [10] L. B. Lucy. ‘A numerical approach to the testing of the fission hypothesis’. In: *The Astronomical Journal* 82.12 (Dec. 1977), pp. 1013–1024. ISSN: 0004–6256. DOI: [10.1086/112164](https://doi.org/10.1086/112164).
- [11] R. A. Gingold and J. J. Monaghan. ‘Smoothed particle hydrodynamics: theory and application to non-spherical stars’. In: *Monthly Notices of the Royal Astronomical Society* 181.3 (Dec. 1977), pp. 375–389. ISSN: 0035–8711. DOI: [10.1093/mnras/181.3.375](https://doi.org/10.1093/mnras/181.3.375).
- [12] T. E. Dushane. ‘Convergence for a Vortex Method for Solving Euler’s Equation’. In: *Mathematics of Computation* 27.124 (Oct. 1973), pp. 719–728. ISSN: 0025–5718. DOI: [10.2307/2005505](https://doi.org/10.2307/2005505).
- [13] O. H. Hald and V. Mauceri Del Prete. ‘Convergence of Vortex Methods for Euler’s Equations’. In: *Mathematics of Computation* 32.143 (July 1978), pp. 791–809. ISSN: 0025–5718. DOI: [10.1090/S0025-5718-1978-0492039-1](https://doi.org/10.1090/S0025-5718-1978-0492039-1).
- [14] O. H. Hald. ‘Convergence of Vortex Methods for Euler’s Equations. II’. In: *SIAM Journal on Numerical Analysis* 16.5 (Oct. 1979), pp. 726–755. ISSN: 0036–1429. DOI: [10.1137/0716055](https://doi.org/10.1137/0716055).
- [15] A. Leonard. ‘Vortex Methods for Flow Simulation’. In: *Journal of Computational Physics* 37.3 (Oct. 1980), pp. 289–335. ISSN: 0021–9991. DOI: [10.1016/0021-9991\(80\)90040-6](https://doi.org/10.1016/0021-9991(80)90040-6).

- [16] A. Leonard. ‘Computing Three-Dimensional Incompressible Flows with Vortex Elements’. In: *Annual Reviews of Fluid Mechanics* 17 (Jan. 1985), pp. 523–559. ISSN: 0066–4189. DOI: [10.1146/annurev.fl.17.010185.002515](https://doi.org/10.1146/annurev.fl.17.010185.002515).
- [17] G.-H. Cottet. ‘A new approach for the analysis of Vortex Methods in two and three dimensions’. In: *Annales de l’Institut Henri Poincaré. Analyse non linéaire* 5.3 (1988), pp. 227–285. ISSN: 0294–1449. DOI: [10.1016/S0294-1449\(16\)30346-8](https://doi.org/10.1016/S0294-1449(16)30346-8).
- [18] M. Kirchhart and S. Obi. ‘A Smooth Partition of Unity Finite Element Method for Vortex Particle Regularization’. In: *SIAM Journal on Scientific Computing* 39.5 (Oct. 2017), A2345–A2364. ISSN: 1064–8275. DOI: [10.1137/17M1116258](https://doi.org/10.1137/17M1116258).
- [19] M. Kirchhart. *On Particles and Splines in Bounded Domains*. Preprint. Jan. 2019. arXiv: [1901.09595](https://arxiv.org/abs/1901.09595) [Math.NA].
- [20] B. Merriman. ‘Particle Approximation’. In: *Vortex Dynamics and Vortex Methods*. Ed. by C. Anderson and C. Greengard. Vol. 28. Lectures in Applied Mathematics. American Mathematical Society, 1991, pp. 481–546. ISBN: 9780821811351.
- [21] P. D. Koumoutsakos. ‘Inviscid Axisymmetrization of an Elliptical Vortex’. In: *Journal of Computational Physics* 138.2 (Dec. 1997), pp. 821–857. ISSN: 0021–9991. DOI: [10.1006/jcph.1997.5749](https://doi.org/10.1006/jcph.1997.5749).
- [22] P. Koumoutsakos, G.-H. Cottet and D. Rossinelli. ‘Flow simulations using particles. Bridging Computer Graphics and CFD’. In: *SIGGRAPH 2008 – 35th International Conference on Computer Graphics and Interactive Techniques*. Los Angeles, California, United States of America. Aug. 2008, pp. 1–73. DOI: [10.1145/1401132.1401166](https://doi.org/10.1145/1401132.1401166).
- [23] C. Mimeau, I. Mortazavi and G.-H. Cottet. ‘Applications of an hybrid particle-grid penalization method for the DNS and passive control of bluff-body flows’. In: *Procedia Computer Science* 108 (2017), pp. 1998–2007. ISSN: 1877–0509. DOI: [10.1016/j.procs.2017.05.031](https://doi.org/10.1016/j.procs.2017.05.031).
- [24] T. Gillis, Y. Marichal, G. S. Winckelmans and P. Chatelain. ‘A 2D immersed interface vortex particle–mesh method’. In: *Journal of Computational Physics* 394 (Oct. 2019), pp. 700–718. ISSN: 0021–9991. DOI: [10.1016/j.jcp.2019.05.033](https://doi.org/10.1016/j.jcp.2019.05.033).
- [25] G.-H. Cottet, J.-M. Entancelin, F. Perignon and C. Picard. ‘High order semi-Lagrangian particle methods for transport equations: numerical analysis and implementation issues’. In: *ESAIM: Mathematical Modelling and Numerical Analysis* 48.4 (July 2014), pp. 1029–1060. ISSN: 0764–583X. DOI: [10.1051/m2an/2014009](https://doi.org/10.1051/m2an/2014009).
- [26] A. Cohen and B. Perthame. ‘Optimal Approximations of Transport Equations by Particle and Pseudoparticle Methods’. In: *SIAM Journal on Mathematical Analysis* 32.3 (2000), pp. 616–636. ISSN: 0036–1410. DOI: [10.1137/S0036141099350353](https://doi.org/10.1137/S0036141099350353).
- [27] G. Russo and J. A. Strain. ‘Fast Triangulated Vortex Methods for the 2D Euler Equations’. In: *Journal of Computational Physics* 111.2 (Apr. 1994), pp. 291–323. ISSN: 0021–9991. DOI: [10.1006/jcph.1994.1065](https://doi.org/10.1006/jcph.1994.1065).
- [28] L. L. Schumaker. *Spline Functions. Basic Theory*. 3rd ed. Cambridge University Press, 2007. ISBN: 0521705126. DOI: [10.1017/CB09780511618994](https://doi.org/10.1017/CB09780511618994).
- [29] J. Douglas Jr., T. Dupont and L. Wahlbin. ‘The Stability in L^q of the L^2 -Projection into Finite Element Function Spaces’. In: *Numerische Mathematik* 23.3 (1974), pp. 193–197. ISSN: 0029–599X. DOI: [10.1007/BF01400302](https://doi.org/10.1007/BF01400302).
- [30] M. Crouzeix and V. Thomée. ‘The Stability in L_p and W_p^1 of the L_2 -Projection onto Finite Element Function Spaces’. In: *Mathematics of Computation* 48.178 (Apr. 1987), pp. 521–532. ISSN: 0025–5718. DOI: [10.2307/2007825](https://doi.org/10.2307/2007825).
- [31] D. Fishelov. ‘A new vortex scheme for viscous flows’. In: *Journal of Computational Physics* 86.1 (Jan. 1990), pp. 211–224. ISSN: 0021–9991. DOI: [10.1016/0021-9991\(90\)90098-L](https://doi.org/10.1016/0021-9991(90)90098-L).

- [32] P. Degond and S. Mas-Gallic. ‘The Weighted Particle Method for Convection–Diffusion Equations. Part 1: The Case of an Isotropic Viscosity’. In: *Mathematics of Computation* 53.188 (Oct. 1989), pp. 485–507. ISSN: 0025–5718. DOI: [10.1090/S0025-5718-1989-0983559-9](https://doi.org/10.1090/S0025-5718-1989-0983559-9).
- [33] P. W. Schroeder, C. Lehrenfeld, A. Linke and G. Lube. ‘Towards computable flows and robust estimates for inf-sup stable FEM applied to the time-dependent incompressible Navier–Stokes equations’. In: *SeMA Journal* 75.4 (Dec. 2018), pp. 629–653. ISSN: 2254–3902. DOI: [10.1007/s40324-018-0157-1](https://doi.org/10.1007/s40324-018-0157-1).
- [34] S. Zalesak. ‘Fully Multidimensional Flux-Corrected Transport Algorithms for Fluids’. In: *Journal of Computational Physics* 31.3 (June 1979), pp. 335–362. ISSN: 0021–9991. DOI: [10.1016/0021-9991\(79\)90051-2](https://doi.org/10.1016/0021-9991(79)90051-2).
- [35] J. H. Verner. ‘Numerically optimal Runge–Kutta pairs with interpolants’. In: *Numerical Algorithms* 53.2–3 (Mar. 2010), pp. 383–396. ISSN: 1017–1398. DOI: [10.1007/s11075-009-9290-3](https://doi.org/10.1007/s11075-009-9290-3).
- [36] A. J. Majda and A. L. Bertozzi. *Vorticity and Incompressible Flow*. Cambridge University Press, Nov. 2001. ISBN: 0521630576.